ELSEVIER

Mechanisms of Development 91 (2000) 189–196

www.elsevier.com/locate/modo

The *Drosophila* gene *abstrakt*, required for visual system development, encodes a putative RNA helicase of the DEAD box protein family

Dietmar Schmucker[a,1,2], Gerd Vorbrüggen[b,2], Paula Yeghiayan[a], Hong Qing Fan[a], Herbert Jäckle[b], Ulrike Gaul[a,*]

[a]*Laboratory of Developmental Neurogenetics, The Rockefeller University, 1230 York Avenue, New York, NY 10021, USA*
[b]*Max-Planck Institut für biophysikalische Chemie, Abteilung Molekulare Entwicklungsbiologie, Am Fassberg, D-37077 Göttingen, Germany*

Received 7 October 1999; received in revised form 5 November 1999; accepted 8 November 1999

Abstract

The molecular mechanisms underlying axonal pathfinding are not well understood. In a genetic screen for mutations affecting the projection of the larval optic nerve we isolated the *abstrakt* locus. *abstrakt* is required for pathfinding of the larval optic nerve, and it also affects development in both the adult visual system and the embryonic CNS. Here we report the molecular characterization of *abstrakt*. It encodes a putative ATP-dependent RNA helicase of the DEAD box protein family, with two rare substitutions in the PTRELA and the RG-D motifs, thought to be involved in oligonucleotide binding: serine for threonine, and lysine for arginine, respectively. Two mutant alleles of *abstrakt* show amino acid exchanges in highly conserved positions. A glycine to serine exchange in the HRIGR motif, which is involved in RNA binding and ATP hydrolysis, results in a complete loss of protein function; and a proline to leucine exchange located between the highly conserved ATPase A and PTRELA motifs results in temperature-sensitive protein function. Both the broad requirement for *abstrakt* gene function and its ubiquitous expression are consistent with a molecular function of the *abstrakt* protein in mRNA splicing or translational control.

Keywords: Drosophila melanogaster; Visual system; Visual system development; Bolwig nerve; Axon guidance; *abstrakt*; DEAD box protein; RNA helicase

1. Introduction

The molecular mechanisms underlying axonal pathfinding are not well understood. In an effort to identify new genes involved in axon guidance in *Drosophila*, genetic screens have been carried out to isolate mutations that disrupt normal axonal growth and guidance using different pathfinding paradigms (Seeger et al., 1993; VanVactor et al., 1993; Salzberg et al., 1994; Kolodziej et al., 1995; Martin et al., 1995), including the developing larval visual system (Schmucker et al., 1997).

The larval visual system consists of a pair of photoreceptive organs, called the Bolwig's organs (BO) and their optic nerves, the Bolwig nerves (BN). Each BO consists of only 12 photoreceptors, unipolar neurons, whose axons fasciculate to form the BN. The BN projects ipsilaterally along the surface of the optic lobe anlagen (OLA), the primordia of the adult optic lobes, from where it leaves the surface and grows towards a small target area in the central brain (Steller et al., 1987; Green et al., 1993; Campos et al., 1995). The growth of the BN proceeds in three phases, during which the nerve changes direction at two intermediate targets, P1 and P2, which are located on the surface of the OLA (Schmucker et al., 1997). In a genetic screen for recessive mutations on the third chromosome that disrupt the BN projection, we isolated mutations in 13 genes that affect the projection in distinct phases of its development, suggesting that different genes and mechanisms are involved at different steps of the projection (Schmucker et al., 1997).

One of the mutations isolated in this screen was *abstrakt* (*abs*). In *abs* mutant embryo defects in BN development become evident shortly after the onset of axon outgrowth. While in wild-type embryos the outgrowing BN axons fasciculate rapidly and project as a tightly fasciculated nerve, *abs* mutant embryos show 2–3 axon bundles, which explore a broad area, show abrupt directional changes and often fail to reach the second intermediate target. Furthermore, the distal-most portions of the BN branches are significantly thicker than in wild-type, containing fine filopodia-like axonal extensions that extend over several cell diameters (Schmucker et al., 1997). In *abstrakt* mutants, the formation

* Corresponding author. Tel.: +1-212-327-7621; fax: +1-212-327-7923.

E-mail address: gaul@rockvax.rockefeller.edu (U. Gaul)

[1] Present address: Howard Hughes Medical Institute, Department of Biological Chemistry, University of California, 675 Circle Drive South, Los Angeles, CA 90095, USA.

[2] D. Schmucker and G. Vorbrüggen contributed equally to this work.

0925-4773/00/$ - see front matter
PII: S0925-4773(99)00298-1

of the BO is normal with respect to both cell number and differentiation, and the OLA and the second intermediate target P2 also appear morphologically intact, thus excluding the possibility that the axonal projection defects are merely a secondary consequence of abnormalities in cell number, cell fate, or tissue organization (Schmucker et al., 1997). These results indicate that *abs* is essential for the directed and fasciculated early outgrowth of the BN, as well as for its navigation at later stages. In the following we describe the genetic analysis of *abstrakt* mutants and their effects in the developing larval and adult visual systems, and we report the molecular characterization of the locus.

2. Results

2.1. Isolation of abs alleles

We originally isolated three mutations in the *abs* locus, one EMS (abs^{IIF1}) and two P element-induced (abs^{P4505}, abs^{P620}) alleles (Schmucker et al., 1997). We showed by P element mobilization using a stable transposase source (Robertson et al., 1988) that the lethality and the BN phenotype of the P4505 chromosome are readily reverted, indicating that the *abs* phenotype is indeed caused by the P insertion (Schmucker et al., 1997). This reversion experiment yielded additional lethal alleles of *abs* (e.g. abs^{45LR7}). The *abs* locus was mapped to the 82A1 region both by chromosome in situ hybridization (BDGP; Miklos and Rubin, 1996) and by complementation with chromosomal deficiencies (*Df(3R)XM3* and *Df(3R)A321R*). The BN phenotype of the P allele is mildly enhanced *in trans* to a deficiency for the region, suggesting that abs^{P4505} represents a hypomorphic mutation, while the phenotypes of the excision allele *45LR7* and of the EMS allele *IIF1* are not enhanced *in trans* to a deficiency. Thus, two alleles represent strong hypomorphic or amorphic mutations. None of the four alleles displays any significant temperature sensitivity.

The further phenotypic analysis of *abs* during post-embryonic development was hampered by the cytological position of the *abs* locus, which is proximal to existing FRT insertions (82B). This location excludes the use of the FRT/FLP technique (Xu and Rubin, 1993) for generating genetic mosaics. We therefore decided to carry out a mutagenesis screen for additional, temperature-sensitive alleles of *abs* (see Section 4). We screened 20 000 mutagenized chromosomes and identified one additional EMS-induced allele (abs^{E2}) with pronounced temperature sensitivity. At 28°C, abs^{E2}/abs^{E2} homozygotes die before the third instar larval stage, whereas at 18°C they continue development through larval and pupal stage and die only as pharate adults. Taking advantage of this temperature-sensitive lethality, we were able to order the different *abs* mutations into the following allelic series: E2 $\ll$ P4505 = P620 $<$ IIF1 = 45LR7 = Def.

2.2. Phenotypic defects in abs mutants

Loss of *abs* function in the embryo leads to severe defects in the pathfinding of BN axons (Schmucker et al., 1997; see above and Fig. 2). Given its role in the establishment of the larval visual system in the embryo, we sought to determine whether *abs* is also required for the development of the adult visual system. This analysis of the postembryonic requirement for *abs* function was made possible by to the isolation of the ts allele abs^{E2}. abs^{E2}/abs^{LR7} transheterozygotes, which survive to the third instar larval stage at 25°C and thus represent a partial loss-of-function situation, were examined for axonal projection defects in their developing adult visual system using 24B10 antibodies, which specifically label photoreceptor axons.

In the wild-type, the photoreceptor axons leave the optic stalk and fan out according to their retinotopic position (Kunes and Steller, 1993; Meinertzhagen and Hanson, 1993; Cutforth and Gaul, 1997). The axons of the outer photoreceptors R1–R6 terminate in the first optic ganglion, the lamina, while the axons of the inner photoreceptors R7 and R8 grow deeper into the brain and terminate in the second optic ganglion, the medulla (Fig. 1A). We find that the overall organization of the retinal projections is disrupted in abs^{E2}/abs^{LR7} animals (Fig. 1B). The fan of retinal projections into the optic lobe is irregular in shape, axons terminate prematurely and often cluster aberrantly. As in the larval visual system, there are no apparent defects in photoreceptor differentiation in the developing adult system under these weak hypomorphic *abs* conditions, since both Elav (data not shown) and Chaoptin (Fig. 1B) are expressed, and the number of ommatidia appears to be normal as well. However, we observe some irregularities in the photoreceptor cell layer, including misrotation of ommatidia, additional photoreceptors, and sometimes fewer photoreceptors (see Fig. 1D), suggesting that *abs* function may be pleiotropic.

This notion is confirmed by the fact that abs^{E2}/abs^{LR7} larvae, apart from their visual system-specific defects, often show melanotic tumors at various positions in their bodies (Fig. 1C), reflecting a broader requirement for *abs* function. *abs* mutant embryos also show abnormal axonal projections in the CNS (see Fig. 1E–G). These defects may be responsible for the embryonic lethality of *abs* mutants.

2.3. Molecular characterization of the abs locus

The P4505 and P620 enhancer trap insertions contain a PZ element (Mlodzik and Hiromi, 1992). This allows the recovery of genomic sequences flanking the P insertion site by plasmid rescue, here 8.0 and 10.5 kb long DNA fragments in the 82A1 genomic region (Fig. 2A). These fragments are contained within a chromosomal walk, which spans the 81F–82A interval (Brönner, 1993). The P element insertion sites were mapped by hybridization to the phage walk and then by sequence analysis of the rescue fragments and of the corresponding genomic fragment. The two P

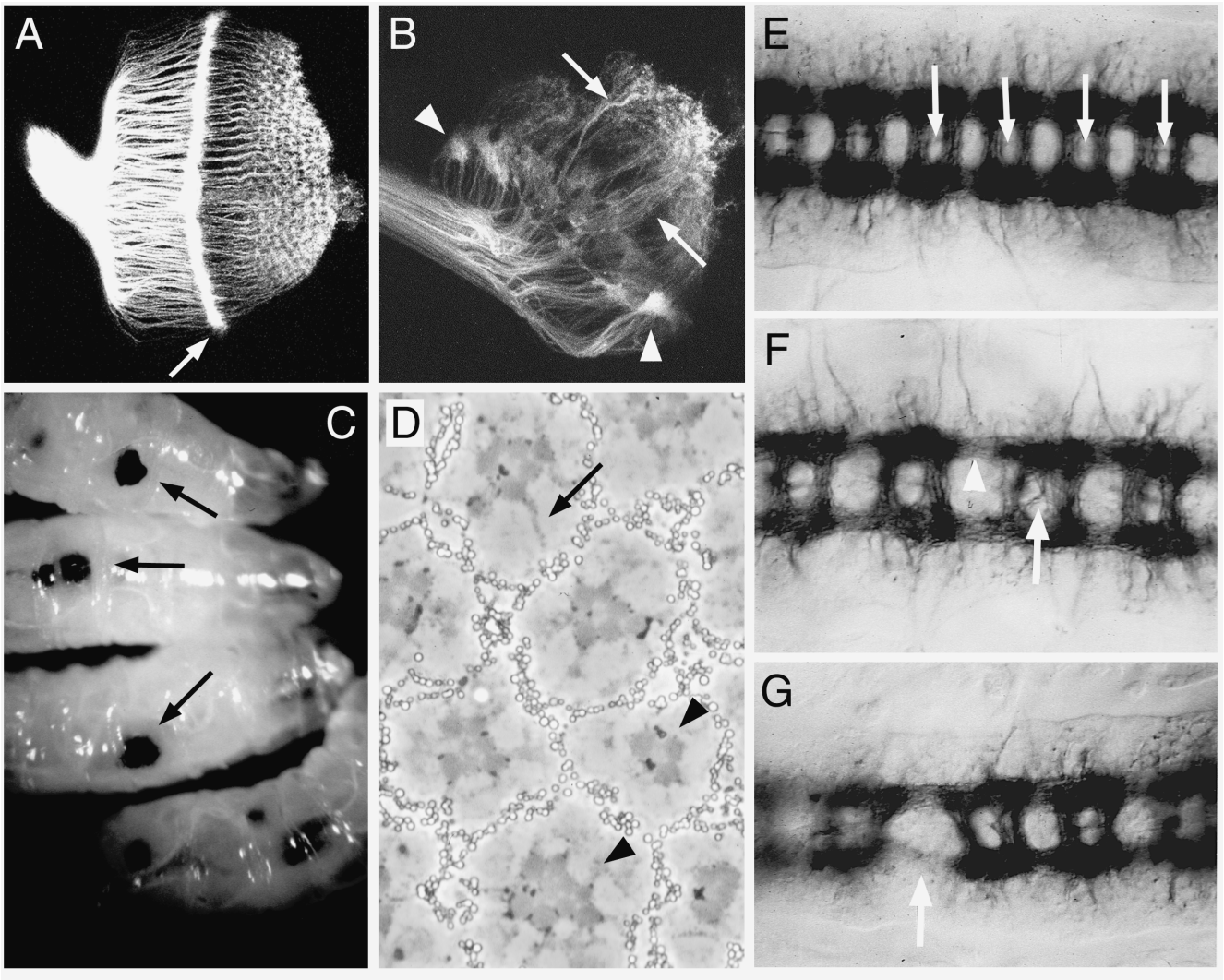

Fig. 1. Phenotypic analysis of *abs* mutants. (A,B) Retinal projections in the developing adult visual system stained with 24B10 antibodies in wild-type (A) and abs^{E2}/abs^{LR7} mutant third instar larvae raised at 25°C (B); posterior view. In wild-type, retinal fibers fan out upon leaving the optic stalk and innervate the lamina in a retinotopic fashion. The projections of the R1–R6 axons terminate in one layer of the lamina (arrow, A). In the *abs* mutant, retinal fibers fail to form an orderly projection into the optic lobe; the termination of fibers in the lamina is very irregular, with fibers lumping together (arrowheads, B) or overshooting into the medulla (arrows, B). (C) abs^{E2}/abs^{LR7} mutant third instar larvae develop melanotic tumors (arrows) at various positions. (D) Adult eye section of $abs^{E2}/absP^{4505}$ mutants raised at 25°C. Several mild abnormalities are observed, including ommatidial rotation defects (arrow) and too few or too many photoreceptors per ommatidium (arrowheads). (E–G) Axonal projections in the embryonic CNS stained with BP102 antibodies in wild-type (E), homozygous mutant abs^{P4505} (F) and abs^{IIF1} (G) embryos; ventral view, anterior to the left. In wild-type, the contralateral axon projections of each segment are entirely bundled into the anterior and posterior commissures; there are no fibers in between (arrows). In *abs* mutants, aberrant fibers can be observed in the intercommissural space (arrow, F) and the connectives are weakened (arrowhead, F) and occasionally even absent (arrow, G). Overall, the CNS appears less compact than in wild-type.

elements are inserted within 9 bp of one another, although in opposite orientation (Fig. 3B). To identify transcripts in the genomic region surrounding the P insertion, we screened cDNA libraries made from embryonic and third instar larval imaginal disc RNA (see Section 4) with a 1.5 kb genomic fragment spanning the P insertion point. We found two non-related families of cDNAs mapping close to the P insertion, cB151 and LD28839 (BDGP; Miklos and Rubin, 1996). To determine the sites of the P insertions relative to the open reading frames (ORFs), we partially sequenced several cDNAs from both transcript families. Comparison of these sequences with the genomic sequences surrounding the P insertion sites revealed that the P620 element had inserted just upstream of the LD28839 transcription unit, while the P4505 element had inserted within it, 17 bp upstream of the first initiation codon, and 774 bp away from the 5′ end of cB151. These findings suggested that LD28839 was the more likely candidate to encode the *abs* locus.

In an attempt to further support this assumption, we examined the expression patterns of the two genes by RNA in situ hybridization. cB151 is expressed ubiquitously at early stages (syncytial blastoderm) and restricted to the mesoderm during stages 8–15 (data not shown), whereas LD28839 is expressed at very low levels throughout devel-

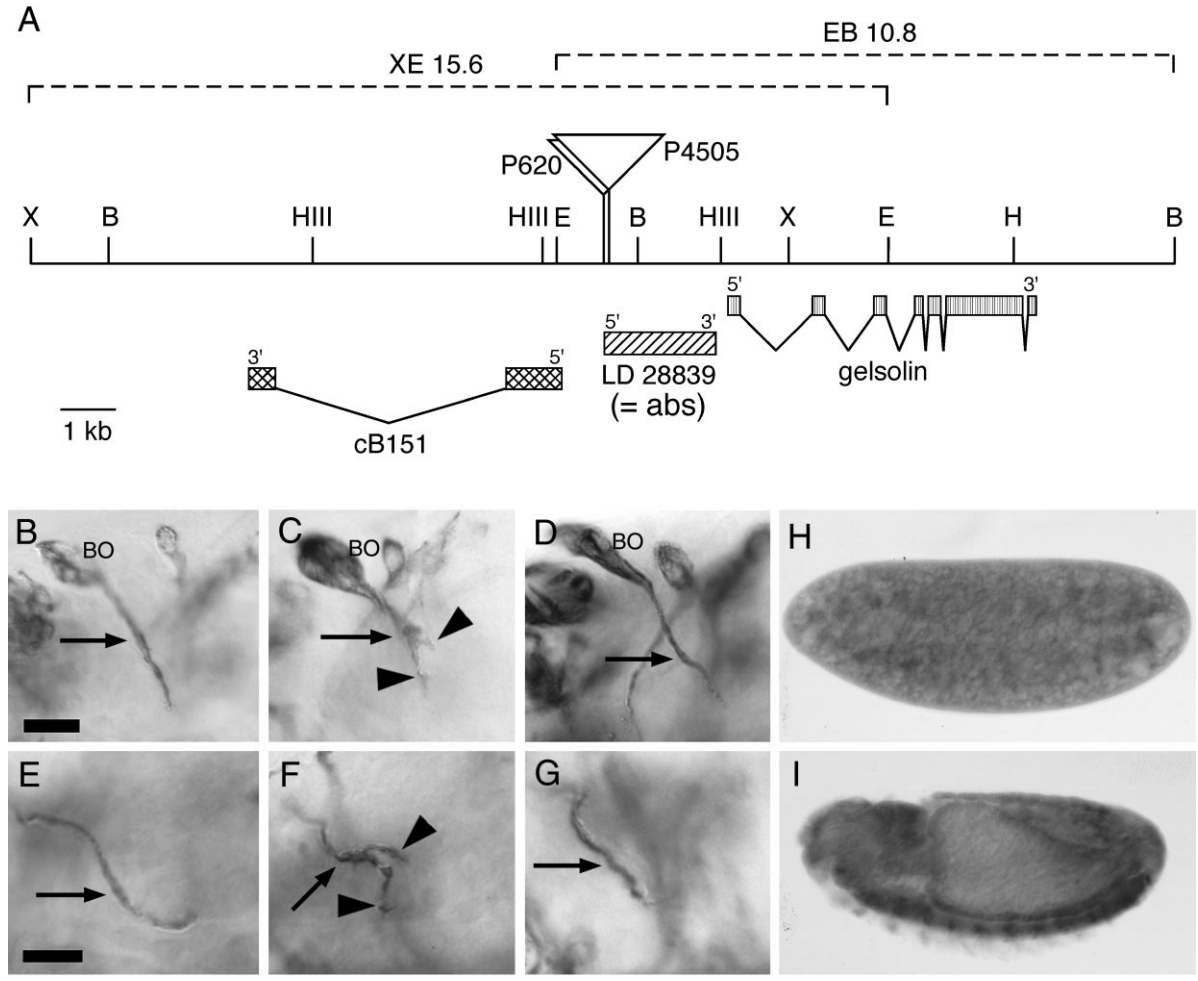

Fig. 2. (A) The genomic region of *abs*. The map shows restriction sites of *Bam*HI (B), *Eco*RI (E), *Hind*III (H) and *Xba*I (X). The P insertions are indicated by triangles. The transcript boundaries are defined by comparison of the cDNA with genomic sequences; the intron–exon boundary of cB151 is estimated by restriction analysis and Southern hybridization. The genomic rescue fragments are indicated as brackets on top. (B–G) Genomic rescue of the Bolwig nerve phenotype. Shown are 22C10 stainings of the BN as it grows along the optic lobe anlage of stage 14 (B–D) and stage 16 (E–G) embryos in a ventrolateral view. In wild-type (B,E), the BN projects as a single nerve (arrow), while in abs^{IIF1}/abs^{45LR7} mutants (C,F) the nerve appears thicker and morphologically abnormal and defasciculates (arrow) into separate branches (arrowheads). In 80% of abs^{IIF1}/abs^{LR7} mutant embryos bearing the XE15.6 genomic rescue fragment the BN projects normally (D,G). (H,I) *abs* RNA in situ hybridization on whole-mount embryos at stage 2 (H) and stage 14 (I); lateral view, anterior to the left. *abs* is expressed ubiquitously at low levels throughout development. Scale bar in (B) for (B–D), and in (E) for (E–G), 20 μm.

opment, and apparently in all tissues (Fig. 2H,I), again suggesting that LD28839 is the more likely candidate. Definitive proof that LD28839 encodes *abs* springs from the analysis of two overlapping genomic rescue fragments, XE15.6 and EB10.8, which both cover LD28839 (Fig. 2A). XE15.6 includes both cB151 and LD28839, while EB10.8 includes both LD28839 and gelsolin, the locus neighboring LD28839 to the right (U. Irion and M. Leptin, unpublished data). XE15.6 and EB10.8 both rescue the lethality of strong allelic combinations of *abs* (abs^{IIF1}/Def) to viability, as well as the axonal pathfinding defects of the BN (Fig. 2B–G), clearly indicating that LD28839 encodes *abs*.

2.4. *abs* encodes a DEAD box protein

We determined the nucleotide sequence of the LD28839 cDNA and found a long open reading frame of 1857 nucleotides. Conceptual translation predicts an 619 residue protein of molecular weight 71 981 (Fig. 3B). The protein is a member of the DEAD box family of ATP-dependent RNA helicases, which includes eIF-4A, p68, Vasa and *Xenopus* An3. Their function as RNA helicases is required to control RNA structure in many cellular processes, in particular mRNA splicing, ribosome assembly and translation initiation (Linder et al., 1989; Schmid and Linder, 1992). The hallmark of this family of proteins is eight highly conserved sequence motifs, whose spacing is well conserved (Schmid and Linder, 1992) (Fig. 3A). These include the ATPase A motif (AxxGxGKT) involved in ATP binding (Walker et al., 1982), the ATPase B (DEAD) involved in ATP hydrolysis (Linder et al., 1989), and the SAT and HRIGR motifs, which are important for helicase and protein–RNA interactions,

respectively (Schmid and Linder, 1991; Pause and Sonnenberg, 1992, 1993; Pause et al., 1993).

In Abs all eight motifs are present in their appropriate spacing (Fig. 3A). Six of the eight motifs are absolutely conserved: the four mentioned above (ATPase A and B, SAT and HRIGR), whose function has been determined, and the GG and TPGR motifs, whose function is not yet known. However, two of the motifs which have been implicated in oligonucleotide binding, PTRELA and RG-D, show conservative substitutions in their amino acid sequence, serine for threonine in the PTRELA motif and lysine for arginine in the RG-D motif. Interestingly, within the large family of DEAD box proteins we have found only two that have the same substitutions, both putative Arabidopsis thalia proteins (At F17M5 and At MWD22). Both proteins show a very high degree of overall sequence similarity with Abs, suggesting that these putative proteins are Abs orthologs. However, nothing is known about the biochemical or biological function of these putative proteins.

To further demonstrate that the DEAD box protein encoded by LD28839 is identical with Abs and to learn more about the structural requirements for Abs protein function, we sequenced the two *abs* mutant alleles that we had isolated in our chemical mutagenesis screens. In the strong loss-of-function allele abs^{IIF1} the absolutely conserved glycine in the HRIGR motif is replaced by a serine. This motif has been shown to be involved in RNA binding and ATP hydrolysis, and mutants in this region have no helicase activity (Pause and Sonnenberg, 1992; Schmid and Linder, 1992; Pause et al., 1993). However, the mutational analysis has so far largely focused on the role of the arginine residues, and the effects of glycine replacements have not been studied. Our finding that the replacement of serine for glycine in the HRIGR motif abrogates Abs function underscores the importance of the strict conservation of this motif and demonstrates that the glycine residue does not tolerate even a conservative change. In the temperature-sensitive partial loss-of-function allele abs^{E2} the proline at position 254 is replaced by leucine. This proline residue is strongly conserved among DEAD box proteins, but does not belong to any of the absolutely conserved sequence motifs. Our finding that a non-conservative exchange of this residue leads to a temperature-sensitive Abs protein product suggests that the proline residue plays an important role for the structure of the protein, either for its activity or for the initial folding of the polypeptide chain during protein synthesis.

3. Concluding remarks

We originally isolated mutations in the *abs* locus in a genetic screen for mutations affecting the projection of the Bolwig nerve. The additional phenotypic analysis uncovers a broader function of *abs* in the embryo, specifically in the development of the CNS, which may be responsible for the lethality of *abs* mutant embryos. Further, during postembryonic stages, *abs* function is not only required in the developing visual system of the adult, but, given the occurrence of melanotic tumors in the mutant, potentially also for the maintenance of normal cellular behavior in a broad range of tissues. For the larval visual system, we have clear evidence that the effects of (zygotic) loss of *abs* function are likely to be due to a direct involvement of the *abs* gene product in axon guidance and not a secondary consequence of abnormalities in cell number, cell fate, or tissue organization (Schmucker et al., 1997). In the developing adult visual system, it is not clear whether *abs* has multiple parallel functions or whether some of the effects we observe are secondary; the molecular role of Abs as a putative RNA helicase does not help to differentiate between these two possibilities. In any case, the broader requirement for *abs* function is consistent with the ubiquitous expression of the *abs* transcript throughout development. Importantly, the *abs* transcript is already present in early embryos prior to the onset of zygotic expression, which is likely to be due to maternally provided RNA. This maternal contribution could potentially mask a requirement for *abs* function both during early and later stages of development. It is therefore possible that embryos lacking both maternal and zygotic *abs* function may show more severe developmental abnormalities. Another question in need of further investigation is the tissue specificity of *abs* requirement.

Our identification of LD28839 as encoding the *abs* gene rests on several lines of evidence. Two lethal P enhancer trap insertions, P620 and P4505 (BDGP; Miklos and Rubin, 1996), which fail to complement the lethality and the BN phenotype of the *abs* point mutations *IIF1* and *E2*, are inserted in the LD28839 transcription unit a few base pairs upstream of the first potential start codon. Secondly, two large genomic rescue fragments which overlap only in the LD28839 genomic region both rescue the lethality and the BN phenotype of *abs* mutants. Finally, both EMS alleles of *abs* have missense mutations in the open reading frame of LD28839, and one of them, *IIF1*, is affecting an absolutely conserved glycine residue in an otherwise highly conserved motif that has been demonstrated to be essential for the function of DEAD box proteins.

DEAD box family members act as ATP-dependent RNA helicases in a number of cellular processes, specifically mRNA splicing, ribosome assembly and translation initiation. The lack of *abs* function leads to a broad range of phenotypic defects, which is compatible with a function of Abs in any of these three processes. Thus, further studies will be required to determine the exact molecular function of the Abs protein during *Drosophila* development. Given its low expression levels, the most promising strategy for elucidating the molecular function of Abs would seem to be by identification of physically interacting proteins, or by identification of mutations that display dominant genetic interactions with *abs*.

The Abs protein shows two amino acid exchanges in two of the highly conserved sequence motifs (PTRELA

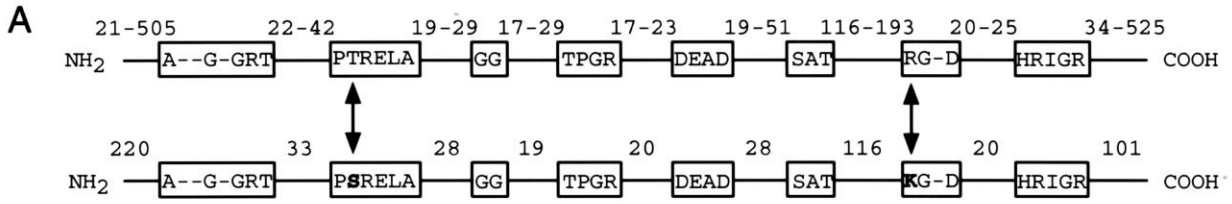
A
21-505
22-42
19-29
17-29
17-23
19-51
116-193
20-25
34-525
NH2
A--G-GRT
PTRELA
GG
TPGR
DEAD
SAT
RG-D
HRIGR
COOH
220
33
28
19
20
28
116
20
101
NH2
A--G-GRT
PSRELA
GG
TPGR
DEAD
SAT
KG-D
HRIGR
COOH

B

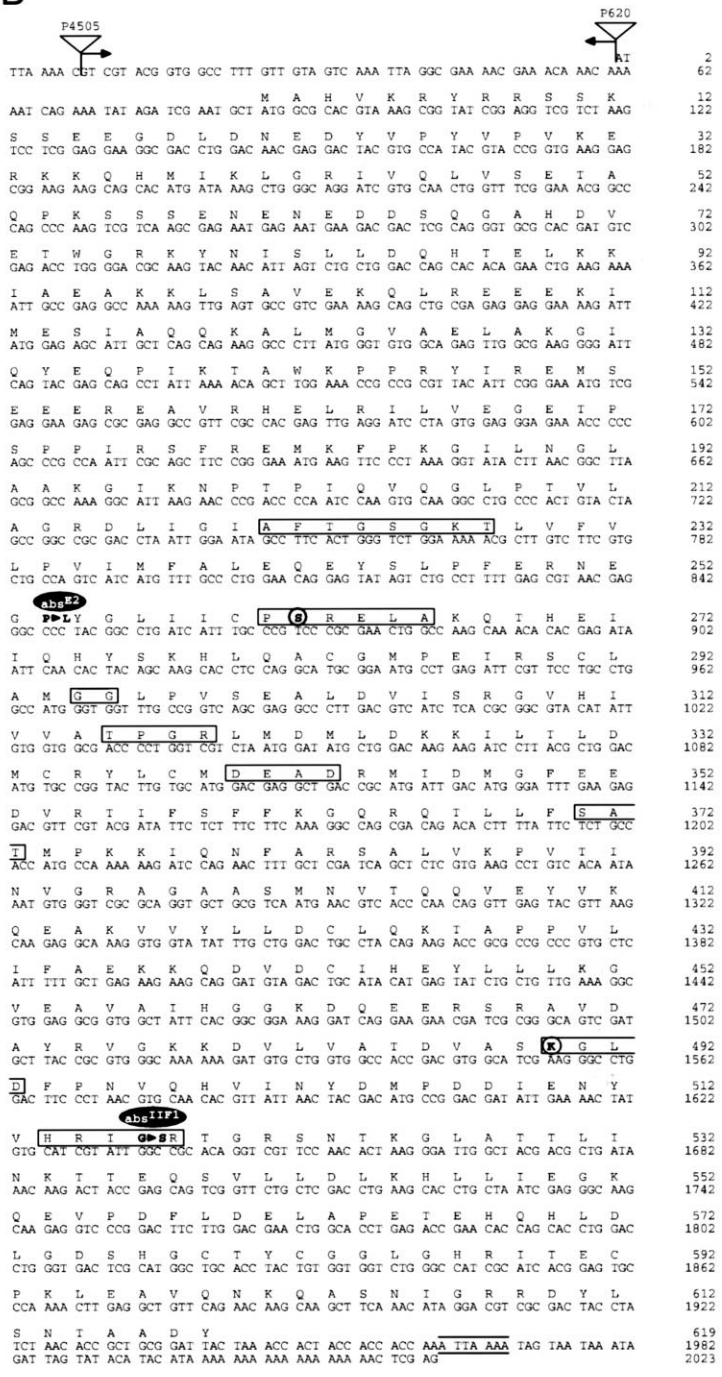
P4505
P620
absE2
absIIF1

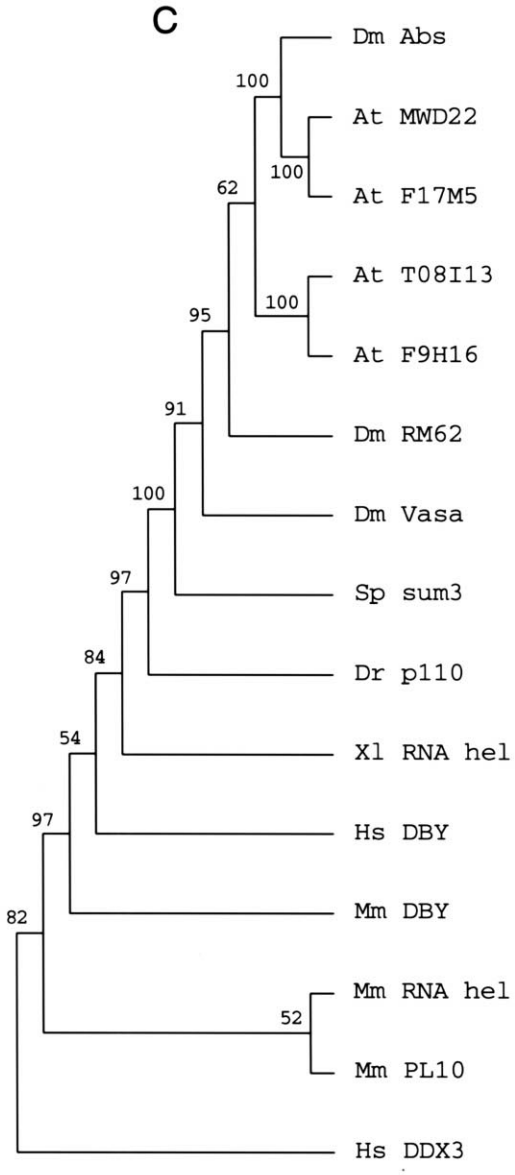
C
Dm Abs
At MWD22
At F17M5
At T08I13
At F9H16
Dm RM62
Dm Vasa
Sp sum3
Dr p110
Xl RNA hel
Hs DBY
Mm DBY
Mm RNA hel
Mm PL10
Hs DDX3
100
100
62
100
95
91
100
97
84
54
97
82
52

and RG-D) that define the RNA helicases of the DEAD box family. These changes have so far been observed only in conjunction, and in only two other proteins of the family, suggesting that this co-variance might be of functional or structural relevance. According to a molecular model of eIF-4A, which is based on the crystal structure of the NS3 helicase of the hepatitis C virus, these two residues appear at close range to one another from opposite sides of an inter-domain cleft in which the residues of the PTRELA and the RG-D motifs are involved in oligonucleotide binding (Subramanya et al., 1996; Benz et al., 1999). Further functional and crystallographic studies will help elucidate the mechanistic implications of the amino acid exchanges found in wild-type and mutant Abs proteins.

4. Experimental procedures

4.1. Isolation of ts alleles of abs

Isogenic *ebony* (*e*) males were mutagenized with EMS and mated en masse to *w; TM3/TM6B, Tb* females. Single *e*/TM6B* males were mated to *abs/TM6B* females and their progeny were raised at 28°C. Non-complementation with *abs* was readily scored by the absence of Tb^+ pupal cases. To determine whether a new allele was ts, stocks of these flies were raised at 18°C and assayed for the presence of Tb^+ larvae.

4.2. Phenotypic analysis and RNA in situ hybridization

Immunocytochemistry of embryos was carried out using standard procedures (Schmucker et al., 1997). The following primary antibodies were used: BP102 (1:10; Seeger et al., 1993); 22C10 (1:50; Fujita et al., 1982); 24B10 (1:200; Zipursky et al., 1984). Detection of primary antibodies was carried out using the ABC-Elite kit (secondary antibodies 1:1000; Vectastain). For confocal microscopy, primary antibodies were detected by FITC- or Cy3-conjugated secondary antibodies (1:100; Jackson). Immunofluorescent images were collected on a Zeiss LSM 510. Whole-mount in situ hybridization of embryos using a digoxygenin-labeled antisense RNA probe of LD38829 was carried out as previously described (Tautz and Peifle, 1989).

4.3. Molecular biology

cDNA libraries prepared from third instar larval eye/antennal discs (constructed by A. Cowman) and from 12–14 h embryos (constructed by N. Brown) were screened using standard methods (Sambrook et al., 1989). A 15.6 kb long *Xba*I–*Eco*RI fragment of genomic DNA was cloned into the pCaspeR4 vector, yielding a rescue construct covering the cB151 and LD28839 genomic regions and the w^+ gene as a transformation marker flanked by P element ends. This construct was injected into w^{1118} *Drosophila* embryos using standard methods (Karess and Rubin, 1984). Strains carrying the 10.8 kb long *Eco*RI–*Bam*HI genomic rescue fragment covering both LD28839 and gelsolin were generously provided by U. Irion and M. Leptin. cDNAs and the corresponding genomic regions were subcloned into pBluescript (Stratagene) for DNA sequencing. DNA was sequenced by the dideoxy chain termination method (Sanger et al., 1977) with vector-specific primers on Applied Biosystems 373A and 377 DNA sequencers (Rockefeller University Protein/DNA Technology Center). Molecular phylogenetic trees were constructed from protein sequence using the PHYLIP 3.572c software based on the parsimony and neighbor joining methods on a Dayhoff distance matrix (PHYLIP (Phylogenetic Interference Package), Version 2.2, J. Felsenstein, Department of Genetics, University of Washington, Seattle, WA). Topology robustness was assessed by 1000 bootstrap resamplings. To identify the molecular defects present in the mutant *abs* alleles, we isolated genomic DNA from flies carrying the mutant chromosomes or the parental *e* chromosome *in trans* to the TM3 balancer, and from *e* homozygous flies. The genomic region containing the entire *abs* ORF was then amplified by PCR (5′ primer GAA AAC CAG AGC ACC TAA AAA located 173 bp upstream of LD28839; 3′ primer GGT TGC TGG GAC GAT TGA TAA located 96 bp downstream of LD28839 polyadenylation signal) and subcloned into the pCR2.1-TOPO vector (Invitrogen) for DNA sequencing. To eliminate PCR artifacts, we carried out three independent PCR reactions and sequenced four different clones for each genotype. The identification of clones containing the mutant *abs* sequences was achieved by comparison with the sequences from the parental and TM3 chromosomes.

Fig. 3. Sequence analysis of the *abstrakt* locus. (A) The organization of conserved sequence motifs in the Abs protein (lower line) as compared to the DEAD box protein consensus (upper line). Abs has all the hallmarks of a DEAD box protein, including a proper spacing of the conserved motifs (Schmid and Linder, 1992). The conservative exchanges in the PTRELA and RG-D motifs are indicated by double arrows. (B) Nucleotide and protein sequence of *abstrakt* (LD28839; GenBank accession number AF212866). Triangles indicate the insertion sites of the P enhancer trap elements; arrows indicate the 5′ to 3′ direction of the P element. The polyadenylation signal is marked by horizontal lines. The conserved sequence motifs are boxed in; the conservative exchanges within the motifs are circled. The amino acid changes of the *abs* mutants are marked by black ovals. (C) Evolutionary relationship of DEAD-box containing proteins, as deduced by neighbor joining analysis. Numbers refer to bootstrap percentages obtained from neighbor-joining. Abstrakt and the Arabidopsis proteins as deduced from the genomic sequences F17M5 and MWD22 are close relatives and candidates for orthologs. At MWD22, accession number AB023044; At F17M5, accession number AL035678; At T08I13, accession number AC002337; At F9H16, accession number AC 007369; Dm RM62 (Dorer et al., 1990); DM Vasa (Lasko and Ashburner, 1988); Sp sum3, accession number AF025536; Dr p110 (Olsen et al., 1997); Xl RNA hel, accession number X57328; Hs DBY (Lahn and Page, 1997); Mm DBY (Mazeyrat et al., 1998); Mm RNA hel (Sowden et al., 1997); Mm PL10 (Leroy et al., 1989); Hs DDX3 (Owsianka and Patel, 1999).

Acknowledgements

We would like to thank Uwe Irion and Maria Leptin for sharing results and materials prior to publication, Lluis Bellsollel and Stephen Burley for molecular modeling of the Abs protein, and members of the Gaul and Jäckle labs for their support and constructive criticism of the project. This work was supported by a fellowship from the Human Frontier Science Program (D.S.), and by grants from the National Institutes of Health (U.G.), the Max-Planck-Society and the Fonds der Chemischen Industrie (H.J.). U.G. is a McKnight Scholar.

References

Benz, J., Trachsel, H., Baumann, U., 1999. Crystal structure of the ATPase domain of translation initiation factor 4A from *Saccharomyces cerevisiae* – the prototype of the DEAD box protein family. Structure 7, 671–679.

Brönner, G., 1993. Untersuchungen zur Struktur, Funktion und Regulation des Gens *huckebein*, eines terminalen Gap-Gen von *Drosophila melanogaster*, Dissertation, Eberhard-Karls-Universität Tübingen, Germany.

Campos, A.R., Lee, K.J., Steller, H., 1995. Establishment of neuronal connectivity during development of the *Drosophila* larval visual system. J. Neurobiol. 28, 313–329.

Cutforth, T., Gaul, U., 1997. The genetics of visual system development in *Drosophila*: specification, connectivity and asymmetry. Curr. Opin. Neurobiol. 7, 48–54.

Dorer, D.R., Christensen, A.C., Johnson, D.H., 1990. A novel RNA helicase gene tightly linked to the Triplo-lethal locus of *Drosophila*. Nucleic Acids Res. 18, 5489–5494.

Fujita, S.C., Zipursky, S.L., Benzer, S., Ferrus, A., Shotwell, S.L., 1982. Monoclonal antibodies against the *Drosophila* nervous system. Proc. Natl. Acad. Sci. USA 79, 7929–7933.

Green, P., Yanoussi-Hartenstein, A., Hartenstein, V., 1993. The embryonic development of the *Drosophila* visual system. Cell Tissue Res. 273, 583–598.

Karess, R.E., Rubin, G.M., 1984. Analysis of P transposable element function in *Drosophila*. Cell 38, 135–146.

Kolodziej, P., Jan, L.Y., Jan, Y.N., 1995. Mutations that affect the length, fasciculation, or ventral orientation of specific sensory axons in the *Drosophila* embryo. Neuron 15, 273–286.

Kunes, S., Steller, H., 1993. Topography in the *Drosophila* visual system. Curr. Opin. Neurobiol. 3, 53–59.

Lahn, B.T., Page, D.C., 1997. Functional coherence of the human Y chromosome. Science 278, 675–680.

Lasko, P.F., Ashburner, M., 1988. The product of the *Drosophila* gene *vasa* is very similar to eukaryotic initiation factor-4A. Nature 335, 611–617.

Leroy, P., Alzari, P., Sassoon, D., Wolgemuth, D., Fellous, M., 1989. The protein encoded by a murine male germ cell-specific transcript is a putative ATP-dependent RNA helicase. Cell 57, 549–559.

Linder, P., Lasko, P.F., Leroy, P., Nielsen, P.J., Nishi, K., Schnier, J., Slonimsky, P.P., 1989. Birth of the DEAD-box. Nature 337, 121–122.

Martin, K., Poeck, B., Roth, H., Ebens, E.J., Conley Ballard, L., Zipursky, S.L., 1995. Mutations disrupting neuronal connectivity in the *Drosophila* visual system. Neuron 14, 229–240.

Mazeyrat, S., Saut, N., Sargent, C.A., Grimmond, S., Longepied, G., Ehrmann, I.E., Ellis, P.S., Greenfield, A., Affara, N.A., Mitchell, M.J., 1998. The mouse Y chromosome interval necessary for spermatogonial proliferation is gene dense with syntenic homology to the human AZFa region. Hum. Mol. Genet. 7, 1713–1724.

Meinertzhagen, I.A., Hanson, T.E., 1993. The development of the optic lobe. In: Bate, M., Martinez-Arias, A. (Eds.). The Development of *Drosophila melanogaster*, Cold Spring Harbor Laboratory Press, Cold Spring Harbor, NY, pp. 1363–1491.

Miklos, G.L.G., Rubin, G.M., 1996. The role of the genome project in determining gene function: insights from model organisms. Cell 86, 521–529.

Mlodzik, M., Hiromi, Y., 1992. Enhancer trap method in *Drosophila*: its application to neurobiology. Methods Neurosci. 9, 397–414.

Olsen, L.C., Aasland, R., Fjose, A., 1997. A vasa-like gene in zebrafish identifies putative primordial germ cells. Mech. Dev. 66, 95–105.

Owsianka, A.M., Patel, A.H., 1999. Hepatitis C virus core protein interacts with a human DEAD box protein DDX3. Virology 257, 330–340.

Pause, A., Sonnenberg, N., 1992. Mutational analysis of a DEAD box RNA helicase: the mammalian translation initiation factor eIF-4A. EMBO J. 11, 2643–2654.

Pause, A., Sonnenberg, N., 1993. Helicases and RNA unwinding in translation. Curr. Opin. Struct. Biol. 3, 953–959.

Pause, A., Methot, N., Sonnenberg, N., 1993. The HRIGRXXR region of the DEAD box RNA helicase eukaryotic translation initiation factor 4A is required for RNA binding and ATP hydrolysis. Mol. Cell. Biol. 13, 6789–6798.

Robertson, H.M., Preston, C.R., Phillis, R.W., Johnson-Schlitz, D., Benz, W.K., Engels, W.R., 1988. A stable source of P-element transposase in *Drosophila melanogaster*. Genetics 18, 461–470.

Salzberg, A., D'Evelyn, D., Schulze, K.L., Lee, J.-K., Strumpf, D., Tsai, L., Bellen, H., 1994. Mutations affecting the pattern of the PNS in *Drosophila* reveal novel aspects of neuronal development. Neuron 13, 269–287.

Sambrook, J., Fritsch, E.F., Maniatis, T., 1989. Molecular Cloning: A Laboratory Manual, Cold Spring Harbor Laboratory Press, Cold Spring Harbor, NY.

Sanger, F., Nicklen, S., Coulson, A.R., 1977. DNA sequencing with chain-terminating inhibitors. Proc. Natl. Acad. Sci. USA 74, 5463–5467.

Schmid, S.R., Linder, P., 1991. Translation initiation factor 4A from *Saccharomyces cerevisiae*: analysis of residues conserved in the D-E-A-D family of RNA helicases. Mol. Cell. Biol. 11, 3463–3471.

Schmid, S.R., Linder, P., 1992. D-E-A-D protein family of putative RNA helicases. Mol. Microbiol. 6, 283–292.

Schmucker, D., Jäckle, H., Gaul, U., 1997. Genetic analysis of the larval optic nerve projection in *Drosophila*. Development 124, 937–948.

Seeger, M., Tear, G., Ferres-Marco, D., Goodman, C.S., 1993. Mutations affecting growth cone guidance in *Drosophila*: genes necessary for guidance toward or away from the midline. Neuron 10, 409–426.

Sowden, J.C., Morrison, K., Putt, W., Beddington, R., Edwards, Y.H., 1997. The identification of novel sequences expressed in the mouse notochord. Mamm. Genome 8, 42–44.

Steller, H., Fischbach, K.F., Rubin, G.M., 1987. *disconnected*: a locus required for neuronal pathway formation in the visual system of *Drosophila*. Cell 50, 1139–1153.

Subramanya, H.S., Bird, L.E., Brannigan, J.A., Wigley, D.B., 1996. Crystal structure of a DExx box DNA helicase. Nature 384, 379–383.

Tautz, D., Peifle, C., 1989. A non-radioactive *in situ* hybridization method for localization of specific RNAs in *Drosophila* embryos reveals translational control of the segmentation gene hunchback. Chromosoma 98, 81–85.

VanVactor, D., Sink, H., Fambrough, D., Tsoo, R., Goodman, C.S., 1993. Genes that control neuromuscular specificity in *Drosophila*. Cell 73, 1137–1153.

Walker, J.E., Saraste, M., Runswick, M.J., Gay, N.J., 1982. Distantly related sequences in the α- and β-subunits of ATP synthase, myosin, kinases and other ATP requiring enzymes and a common nucleotide binding fold. EMBO J. 1, 945–956.

Xu, T., Rubin, G.M., 1993. Analysis of genetic mosaics in developing and adult *Drosophila* tissues. Development 117, 1223–1237.

Zipursky, S.L., Venkatesh, T.R., Teplow, D.B., Benzer, S., 1984. Neuronal development in the *Drosophila* retina: monoclonal antibodies as molecular probes. Cell 36, 15–26.